今日の治療指針

Volum
53

私はこう治療している

総編集
山口　徹　北原光夫　福井次矢

医学書院

(クラミジア，淋菌感染症など）の増加が問題視されている．主症状は月経遅延（無月経），不正性器出血，下腹痛などである．

従来，出血性ショックを呈する女性の急性腹症の代表的疾患とされているが，近年の高感度妊娠検査薬と経腟超音波検査法の普及により早期に診断されることが多くなった．正常妊娠では，妊娠反応は妊娠4週以降ほぼ陽性になり，妊娠5週には経腟超音波で子宮内に胎嚢が確認されてくる．これを考慮して，妊娠反応陽性で子宮腔内に胎嚢が確認されない場合や，子宮外に胎嚢様構造物を認める場合には本疾患を疑う．

治療方針

Ⓐ 手術療法

卵管破裂や出血性ショックを呈している場合は，緊急開腹手術（主に卵管切除術）が行われる．卵管未破裂症例や循環動態が落ち着いている場合には腹腔鏡下手術が選択され，腹腔鏡下に卵管線状切開術や卵管切除術を行う．挙児希望があり，腫瘤径5 cm未満，血中ヒト絨毛性ゴナドトロピン（hCG）値10,000 IU/L以下，初回卵管妊娠，胎児心拍陰性，未破裂症例には卵管線状切開術の適応となる．

Ⓑ 薬物療法

活動性出血がなく循環動態が安定している卵管未破裂症例で，未破裂腫瘤の最大径が3－4 cm未満，血中hCG値が3,000－5,000 IU/L未満の場合には薬物療法が選択されることがある．薬物としてはメトトレキサート（MTX）の全身投与法と超音波ガイド下の胎嚢内局所投与法とがある．しかし，手術療法に比べてその有効性は低いとされている．また，いずれも保険適用外である．

Ⓒ 待機療法

臨床症状に乏しく，血中hCG値が1,000 IU/L未満でかつ低下傾向にある場合，自然寛解が得られることがある．ただし，血中hCG値が迅速に測定でき，緊急手術が可能な状態でのフォローが前提とされる．

患者説明のポイント

- 妊娠反応陽性で子宮腔内に胎嚢を認めない場合，正常初期妊娠，流産，異所性妊娠の鑑別が必要であり，経時的に血中hCG値測定や経腟超音波検査を行う．
- 卵管温存手術は卵管切除術に比べて次回妊娠（自然妊娠）に対し有効ではあるが，同側の異所性妊娠率（再発率）は約18%と決して低くない（日産婦誌59巻6号）ことを説明する．
- 待機療法や薬物療法を行う場合には腹腔内出血による緊急手術，異所性妊娠の存続，絨毛性疾患を念頭に置く必要がある．また，経過観察中に症状の増悪を認めた場合は早急に受診する旨を説明する．

絨毛性疾患
trophoblastic disease

片渕秀隆　熊本大学大学院教授・産科婦人科学

病態と診断

絨毛性疾患とは，絨毛細胞の異常増殖によって生じる疾患の総称であり，胞状奇胎，絨毛癌，存続絨毛症，placental site trophoblastic tumor（PSTT），epithelioid trophoblastic tumor（ETT）などがこれに含まれる．

Ⓐ 胞状奇胎

胞状奇胎は，すべての絨毛が嚢胞化して認められる全胞状奇胎と一部の絨毛が嚢胞化し胎芽ないし胎児成分の存在する部分胞状奇胎の2つに分類される．また，これらの胞状奇胎が子宮筋層へ侵入するものを侵入奇胎，肺などに転移するものを転移奇胎という．全胞状奇胎は雄核発生をその起源とし，部分胞状奇胎は3倍体からなる．ヒト絨毛性ゴナドトロピン（human chorionic gonadotropin：hCG）を産生する絨毛細胞の異常な増殖を反映して，尿中ならびに血中のhCG値が高値を示し，超音波断層法で子宮腔内に多数の嚢胞パターン（vesicle pattern）が認められる．診断は摘出標本の肉眼的ならびに病理組織学的所見によって決定される．

Ⓑ 絨毛癌

絨毛癌は異型を示す絨毛細胞が増殖する悪性腫瘍で，組織学的に合胞体栄養膜細胞，細胞性栄養膜細胞および中間型栄養膜細胞と認識される細胞からなり，絨毛形態を認めないものをいい，病理組織学的に診断する．胞状奇胎の既往例に絨毛癌の発症が多くみられるが，既往のない症例にも認められる．また，まれながら妊娠時の胎盤内に原発する胎盤内絨毛癌も存在する．

Ⓒ 存続絨毛症

胞状奇胎の加療後に尿中あるいは血中のhCG値の下降が不良で，画像検査によって侵入奇胎，転移奇胎や絨毛癌が疑われるが，組織学的な診断が得られない場合に，わが国では絨毛癌診断スコア（表）を用いて臨床的に評価する．すなわち，4点以下を臨床的侵入奇胎もしくは臨床的転移奇胎，5点以上を臨床的絨毛癌とする．画像検査で病巣がとらえられない場合には，奇胎後hCG存続症とする．

表　絨毛癌診断スコア

スコア	0	1	2	3	4	5
先行妊娠	胞状奇胎	―	―	流産	―	満期産
潜伏期	－6か月	―	―	―	6か月－3年	3年－
原発病巣	子宮体部 子宮傍結合織 膣	―	―	卵管 卵巣	子宮頸部	骨盤外
転移部位	なし・肺 骨盤内	―	―	―	―	骨盤外 （肺を除く）
肺転移巣 直径 大小不同性 個数	 －20 mm なし －20	 ― ― ―	 ― ― ―	 20－30 mm ― ―	 ― あり ―	 30 mm－ ― 20－
尿中hCG	-10^6 IU/L	10^6-10^7 IU/L	―	10^7 IU/L－	―	―
基礎体温	不規則・一相性	―	―	―	―	二相性

合計スコア：4点以下　臨床的侵入奇胎・転移奇胎，5点以上　臨床的絨毛癌
（日本産科婦人科学会・日本病理学会編：絨毛性疾患取扱い規約．p13，金原出版，1995より転載）

Ⓓ PSTT，ETT

いずれも中間型栄養膜細胞から発生するまれな腫瘍である．絨毛癌とは異なり合胞体ならびに細胞性栄養膜細胞の増生を一般に伴わないために血中hCG値は比較的低値を示す．

治療方針

胞状奇胎の治療は，子宮内容除去術が基本であり，診断が確定した場合には1週間後に再度施行する．組織学的診断による侵入奇胎や絨毛癌診断スコアに基づいた臨床的侵入奇胎や臨床的転移奇胎，奇胎後hCG存続症では，メトトレキサートを主体とした化学療法を行う．また，メトトレキサートの副作用を軽減させるためにロイコボリンによる救援療法を追加することがある．

これらの治療に抵抗を示す場合や多発する転移部位を有する臨床的転移奇胎，組織学的あるいは臨床的絨毛癌では，メトトレキサートにアクチノマイシンDを併用するMA療法，MA療法にシクロホスファミドを加えるMAC療法やエトポシドを加えるMEA療法，さらにこれらの4剤にビンクリスチンを加えるEMACO療法が用いられる．

化学療法は基本的に，血中hCG値が測定感度以下になったあとに2コースを追加し終了とする．また，化学療法に抵抗性を示す症例においては，手術療法や放射線療法を併用する．特に，PSTTやETTでは化学療法抵抗性を示すことが多く，この場合は手術療法が中心となる．

絨毛性疾患の診断ならびに治療の国際的な比較のために2000年に国際産婦人科連合（International Federation of Gynecology and Obstetrics：FIGO）によってgestational trophoblastic neoplasiaの分類が提唱されており，今後EBM（evidence－based medicine）を目指した国際的分類に基づく大規模臨床試験が期待される．

1. メトトレキサート（MTX）療法

℞ 処方例

メソトレキセート注　1回0.4 mg/kg　1日1回　筋注　4日間連続　休薬期間7日間

2. メトトレキサート（ロイコボリン救援）〔MTX（LV）〕療法

℞ 処方例

メソトレキセート注　1回1.0 mg/kg　1日1回，ロイコボリン注　MTXの1/10量　1日1回　それぞれ隔日に4回　筋注　休薬期間7日間

3. メトトレキサート・アクチノマイシンD（ロイコボリン救援）〔MA（LV）〕療法

℞ 処方例　2.MTX（LV）療法の処方例に下記を加える．

コスメゲン注　1回10 μg/kg　1日1回　静注　4日間連続　休薬期間10－14日

4. エトポシド・メトトレキサート・アクチノマイシンD・シクロホスファミド・ビンクリスチン（EMACO）療法

a. コース1

℞ 処方例

1日目：

ベプシド注　1回100 mg/m² 30分以上かけて点滴静注

メソトレキセート注　1回 300 mg/m² 12時間かけて点滴静注（1回 100 mg/m² 静注と1回 200 mg/m² 点滴静注に分けても可能）
コスメゲン注　1回 0.5 mg/body　静注
2日目：
ベプシド注　1回 100 mg/m²　30分以上かけて点滴静注
コスメゲン注　1回 0.5 mg/body　静注
ロイコボリン注　1回 15 mg/body　筋注
MTX 投与開始 24 時間後から 12 時間おきに4回投与

b. コース2

℞ 処方例

エンドキサン注　1回 600 mg/m²　1日1回　静注
オンコビン注　1回 1.0 mg/m²　1日1回　静注
6日間隔でコース1，2を交互に投与する．

高年初産婦
elderly primipara

増﨑英明　長崎大学教授・産科婦人科学

病態と診断

高年初産婦とは35歳以上の女性が初めて妊娠したものをいう．高齢妊娠はいくつかのリスクを有するが，それは30歳を超えた頃から徐々に高まるものであり，35歳から突然に危険性が増すというものではない．

高齢出産の年度別推移をみると，1970年代はおよそ5%であったが，1990年代は10%に増加した．2000年以降は急速に増加して2008年には20%を超えて出産総数のおよそ1/5を占めるまでになっている．厚労省の統計によれば，2005年に40歳以上での出産は2万人を超えている．

高年初産婦の有する危険は，高齢妊娠に由来するものと高齢分娩によるものに分けることができる．ただし，高年初産婦の多くは正常な妊娠・分娩で経過しており，高年初産婦が絶対的に危険というのではなく，若いうちに比べると相対的に危険性が高まるという意味である．

治療方針

Ⓐ 妊娠中の危険性

高齢になると卵子の質は次第に劣化する．また染色体異常の頻度は増加する．染色体異常のうち21トリソミーの頻度は，母親の年齢が20代前半ではおよそ1/1,500であるが，35歳で1/400，40歳では1/100程度になる．また染色体異常の増加に伴って，高齢妊娠では流産の頻度も増えるので，希望者には遺伝カウンセリングが必要なこともある．そのほか，高齢妊娠では妊娠高血圧症候群や妊娠糖尿病などの合併妊娠に注意する．さらに子宮頸癌や乳癌などの好発年齢にあたるので，子宮癌検診や乳癌検診も必要である．

Ⓑ 分娩時の危険性

高年初産婦では，軟産道強靭，微弱陣痛や分娩遷延，子宮筋腫合併などの頻度が高く，帝王切開による分娩が増加する．大量出血による危険性も若年者より高い．結果的に母体死亡や周産期死亡の危険も相対的に高い．そのため高次施設での妊娠管理や分娩管理が望ましいとの意見も少なくない．

患者説明のポイント

・母体の年齢と染色体異常発生率，妊娠高血圧症候群に対する注意，帝王切開分娩の可能性などについて説明する．高次施設での分娩の可能性について話し合うことも大事である．

合併症妊娠
medical complications during pregnancy

上妻志郎　東京大学大学院教授・分子細胞生殖医学

病態と診断

合併症が妊娠に及ぼす影響としては流早産，妊娠高血圧症候群，胎児発育および機能障害，胎児死亡など，妊娠が合併症に及ぼす影響としては，母体の各種臓器障害，母体死亡がある．妊娠した場合には，それに気付くまでに妊娠状態が1か月以上継続していることが多く，気付いたときにはすでに相互の影響が生じ，心疾患・糖尿病などが急速に悪化したり，胎児形態異常が発生したりすることがある．したがって，合併症を有し妊娠を希望する場合には，妊娠する前に合併症の評価と必要に応じた治療をしておくことが好ましい．近年，中等度以上の合併症を有する女性に対する不妊症治療の是非が問題となっている．いずれの場合においても，各専門医と緊密に連絡を取り合い，迅速かつ総合的な判断が必要とされる．

治療方針

Ⓐ 心疾患

心疾患の種類と程度によっては高率に母体死亡に至り，母体死亡の8%を占めるといわれる．肺高血圧症，弁病変を伴う大動脈縮窄症，大動脈病変を伴うMarfan症候群では特に高率である．

New York Heart Association（NYHA）の心機能分類のIII，IVでは心不全の病期にあると判断さ

CLINICAL REPORT

AMERICAN JOURNAL OF medical genetics PART A

Aberrant Methylation of H19-DMR Acquired After Implantation Was Dissimilar in Soma Versus Placenta of Patients With Beckwith–Wiedemann Syndrome

Ken Higashimoto,[1] Kazuhiko Nakabayashi,[2] Hitomi Yatsuki,[1] Hokuto Yoshinaga,[1] Kosuke Jozaki,[1] Junichiro Okada,[3] Yoriko Watanabe,[3] Aiko Aoki,[4] Arihiro Shiozaki,[4] Shigeru Saito,[4] Kayoko Koide,[1] Tsunehiro Mukai,[5] Kenichiro Hata,[2] and Hidenobu Soejima[1]*

[1]Division of Molecular Genetics & Epigenetics, Department of Biomolecular Sciences, Faculty of Medicine, Saga University, Saga, Japan

[2]Department of Maternal–Fetal Biology, National Research Institute for Child Health and Development, Setagaya, Tokyo, Japan

[3]Department of Pediatrics, Kurume University, Kurume, Japan

[4]Department of Obstetrics and Gynecology, University of Toyama, Toyama, Japan

[5]Nishikyushu University, Kanzaki, Saga, Japan

Received 7 October 2011; Accepted 19 January 2012

Gain of methylation (GOM) at the H19 differentially methylated region (H19-DMR) is one of several causative alterations in Beckwith–Wiedemann syndrome (BWS), an imprinting-related disorder. In most patients with epigenetic changes at H19-DMR, the timing of and mechanism mediating GOM is unknown. To clarify this, we analyzed methylation at the imprinting control regions of somatic tissues and the placenta from two unrelated, naturally conceived patients with sporadic BWS. Maternal H19-DMR was abnormally and variably hypermethylated in both patients, indicating epigenetic mosaicism. Aberrant methylation levels were consistently lower in placenta than in blood and skin. Mosaic and discordant methylation strongly suggested that aberrant hypermethylation occurred after implantation, when genome-wide de novo methylation normally occurs. We expect aberrant de novo hypermethylation of H19-DMR happens to a greater extent in embryos than in placentas, as this is normally the case for de novo methylation. In addition, of 16 primary imprinted DMRs analyzed, only H19-DMR was aberrantly methylated, except for *NNAT* DMR in the placental chorangioma of Patient 2. To our knowledge, these are the first data suggesting when GOM of H19-DMR occurs.

Key words: Beckwith–Wiedemann syndrome; H19-DMR; aberrant DNA methylation; after implantation

How to Cite this Article:
Higashimoto K, Nakabayashi K, Yatsuki H, Yoshinaga H, Jozaki K, Okada J, Watanabe Y, Aoki A, Shiozaki A, Saito S, Koide K, Mukai T, Hata K, Soejima H. 2012. Aberrant methylation of H19-DMR acquired after implantation was dissimilar in soma versus placenta of patients with Beckwith–Wiedemann syndrome.
Am J Med Genet Part A 9999:1–6.

INTRODUCTION

Beckwith–Wiedemann syndrome (BWS) is an imprinting-related condition characterized by macrosomia, macroglossia, and abdominal wall defects (OMIM #130650). The relevant imprinted chromosomal region in BWS, 11p15.5, consists of two independent imprinted domains, *IGF2/H19* and *CDKN1C/KCNQ1OT1*. Imprinted genes within each domain are regulated by two imprinting control regions (ICR), the H19-differentially methylated region (DMR) or KvDMR1 [Weksberg et al., 2010]. Several causative alterations have been identified in patients with BWS: loss of methylation (LOM) at KvDMR1, gain of methylation (GOM) at H19-DMR, paternal uniparental disomy (UPD), *CDKN1C* mutations, and chromosomal abnormality involving 11p15 [Sasaki et al., 2007; Weksberg et al., 2010].

Additional supporting information may be found in the online version of this article.

Grant sponsor: Japan Society for the Promotion of Science; Grant number: 20590330; Grant sponsor: Ministry of Health, Labor, and Welfare; Grant sponsor: National Center for Child Health and Development.

*Correspondence to:
Hidenobu Soejima, Professor[Q1], Division of Molecular Genetics & Epigenetics, Department of Biomolecular Sciences, Faculty of Medicine, Saga University, 5-1-1 Nabeshima, Saga 849-8501, Japan.
E-mail: soejimah@med.saga-u.ac.jp

Published online 00 Month 2012 in Wiley Online Library (wileyonlinelibrary.com).
DOI 10.1002/ajmg.a.35335

Methylation of H19-DMR is erased in primordial germ cells (PGCs) but becomes reestablished during spermatogenesis [Li, 2002; Sasaki and Matsui, 2008]: this methylation regulates the expression of *IGF2* and *H19* by functioning as a chromatin insulator, restricting access to shared enhancers [Bell and Felsenfeld, 2000; Hark et al., 2000]. GOM on the maternal H19-DMR leads to expression of both *IGF2* alleles and silencing of both *H19* alleles. Dominant maternal transmissions of microdeletions and/or base substitutions within H19-DMR have recently been reported in a few patients of BWS with H19-DMR GOM [Demars et al., 2010]. However, when and how the GOM on the maternal H19-DMR occurs is not clear.

Here, we found epigenetic mosaicism in two BWS patients. We also found that GOM at H19-DMR was discordant in blood and skin versus placenta; specifically, methylation levels were lower in placental samples. These findings strongly suggest that aberrant methylation of H19-DMR occurred after implantation. As a result, we expect aberrant de novo methylation happens to a greater extent in embryos than in placentas.

MATERIALS AND METHODS

Patients

Two unrelated patients with sporadic BWS, Patient 1 (BWS047) and Patient 2 (bwsh21-015), were delivered by cesarean in the third trimester of pregnancy. The mothers of both patients conceived naturally. Patient 1 and Patient 2 met clinical criteria for BWS as described by Elliott et al. [1994] and Weksberg et al. [2001], respectively (Table I). The placenta of Patient 1 was large and weighed 1,065 g, but was without any pathological abnormality. The placenta of Patient 2 was also large, weighing 1,620 g, and had an encapsulated placental chorangioma, as reported previously [Aoki et al., 2011]. The standard G-banding chromosome analysis using peripheral blood samples showed no abnormalities in either patient. This study was approved by the Ethics Committee for Human Genome and Gene Analyses of the Faculty of Medicine, Saga University.

Southern Blot Analysis

Genomic DNA was extracted from embryo-derived somatic tissues and the placentas of the patients (Fig. 1). Methylation-sensitive Southern blots with *Bam*HI and *Not*I were employed for KvDMR1, and blots with *Pst*I and *Mlu*I were employed for H19-DMR, as described previously [Soejima et al., 2004]. Band intensity was measured using the FLA-7000 fluoro-image analyzer (Fujifilm[Q2], Japan). The methylation index (MI, %) was then calculated (Fig. 1). Southern blots with *Apa*I were used to identify the microdeletion of H19-DMR as described previously [Sparago et al., 2004].

Bisulfite Sequencing and Combined Bisulfite Restriction Analysis (COBRA)

Bisulfite sequencing covering the sixth CTCF binding site (CTS6) was performed. For COBRA, PCR products of each primary imprinted DMR were digested with the appropriate restriction endonucleases and were then separated using the MultiNA Microchip Electrophoresis System (Shimazdu, Japan). The methylation index was also calculated. All PCR primer sets used in this study have been listed in Supplementary Table SI (See Supporting Information online).

DNA Polymorphism Analyses

For quantitative polymorphism analyses, tetranucleotide repeat markers (*D11S1997* and *HUMTH01*) and a triplet repeat marker (*D11S2362*) from 11p15.4–p15.5 were amplified and separated by electrophoresis on an Applied Biosystems 3130 genetic analyzer (Applied[Q3] Biosystems); data were quantitatively analyzed with the GeneMapper software. The peak height ratios of paternal allele to maternal allele were calculated. A single nucleotide polymorphism (SNP) for the *Rsa*I recognition site in *H19* exon 5 (rs2839703) was also quantitatively analyzed using hot-stop PCR [Uejima et al., 2000]. Band intensity was measured using the FLA-7000 fluoro-image analyzer (Fujifilm).

Mutation Search of H19-DMR

To search for mutations in the binding sites of CTCF, OCT4, and SOX2, we sequenced a genomic region in and around H19-DMR, which included seven CTCF-binding sites, three OCT4 sites, and one SOX2 site.

TABLE I. Clinical Information of BWS Patients

Patient ID	Conception	Birth weight (gestational age)	Clinical features	Karyotype	Placental weight and pathology	Placental–fetal weight ratio
Patient 1 (BWS047)	Natural	4,506 g (36w2d)	Macrosomia macroglossia abdominal wall defect hypoglycemia	46,XY	1,065 g no pathological findings	0.236
Patient 2 (bwsh21-015)	Natural	2,540 g (33w5d)	Macrosomia macroglossia hypoglycemia renal malformation hepatosplenomegaly	46,XX	1,620 g placental chorangioma	0.638

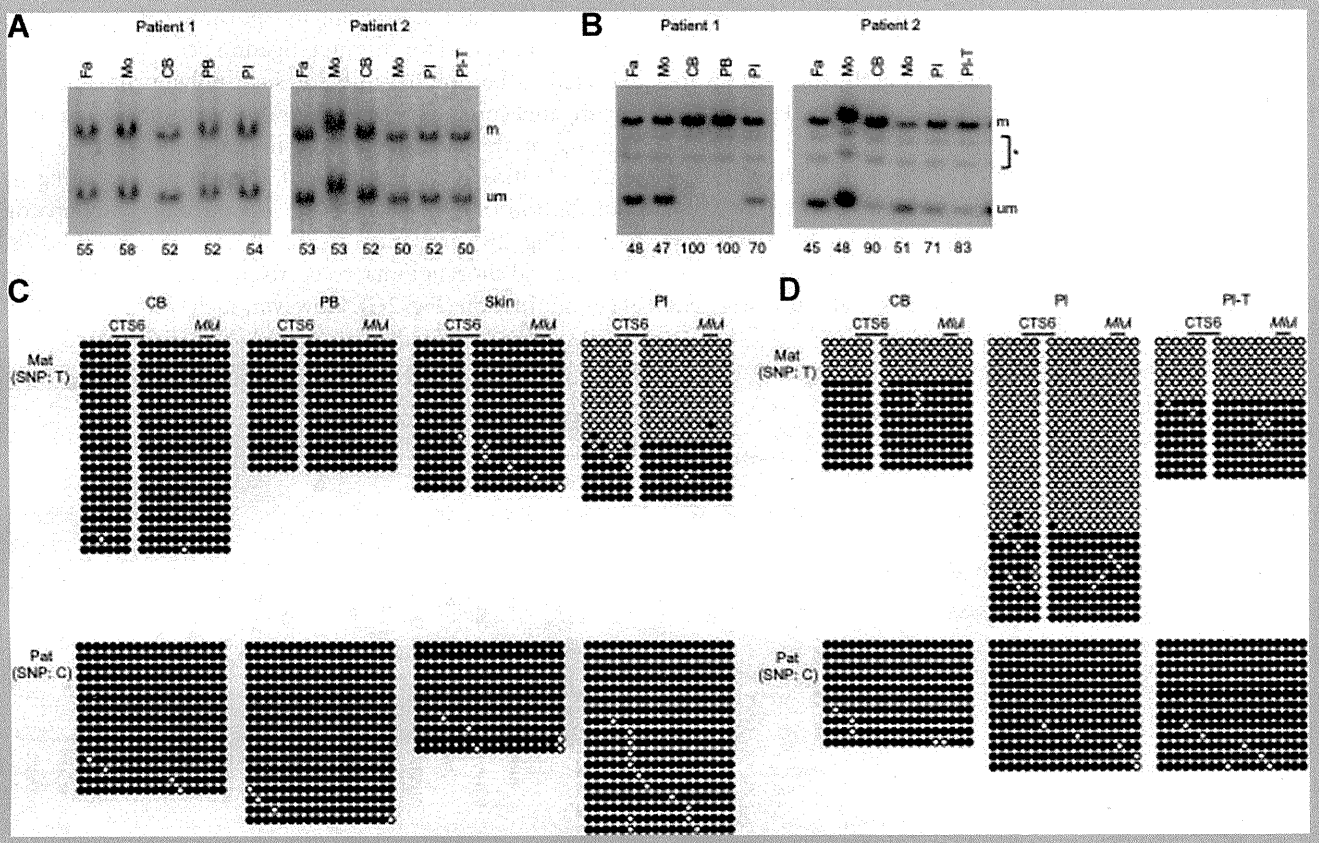

FIG. 1. Methylation analyses of KvDMR1 and H19-DMR. A: Methylation-sensitive Southern blots for KvDMR1. Genomic DNA was extracted from the cord blood, peripheral blood, skin, and placenta of Patient 1 and from the cord blood, placenta, and placental chorangioma of Patient 2. Methylation at KvDMR1 was normal in all samples analyzed. Methylation indices (MI, %) are shown under the figure. B: Methylation-sensitive Southern blots for H19-DMR. The MIs of blood samples were higher than the MIs of placental samples. MI was calculated using the equation [M/(M + U)] × 100, where M is the intensity of the methylated band and U is the intensity of the unmethylated band. C: Bisulfite sequencing of H19-DMR in Patient 1. The two parental alleles were distinguishable by differences in SNPs. Both parental alleles were completely methylated in the cord blood, peripheral blood, and skin samples, and the maternal allele, which is normally unmethylated, was partially methylated in the placenta. D: Bisulfite sequencing of H19-DMR in Patient 2. Methylation of the maternal allele was higher in the cord blood than in the placenta or placental chorangioma. These results were consistent with the results of the Southern blot analysis. We confirmed complete methylation of paternal H19-DMR alleles and complete demethylation of maternal H19-DMR alleles in four normal control placentas that were heterozygous for identifiable SNPs (data not shown). Fa, father; Mo, mother; CB, cord blood; PB, peripheral blood; Pl, placenta; Pl-T, placental chorangioma; m, methylated band; um, unmethylated band; *, nonspecific bands; Mat, maternal allele; Pat, paternal allele; CTS6, sixth CTCF binding site; *MluI*, a restriction site approximately 80 bp downstream of CTS6 assayed by methylation-sensitive Southern blot and COBRA.

RESULTS

We first examined the methylation status of the two ICRs, KvDMR1, and H19-DMR, at 11p15.5 using methylation-sensitive Southern blot analysis. Methylation at KvDMR1 was normal in all samples collected (Fig. 1A); however, methylation at H19-DMR was aberrant (Fig. 1B). In Patient 1, hypermethylation at H19-DMR was complete in cord blood and peripheral blood samples (MI = 100%), and hypermethylation in the placenta was partial (MI = 70%). In Patient 2, H19-DMR was partially hypermethylated in cord blood (MI = 90%) but less so in the placenta and placental chorangioma (MI = 71% and MI = 83%, respectively). For further investigation of differences in methylation between the patients' somatic tissues and placentas, the CTS6 site was subjected to bisulfite sequencing (Fig. 1C and D). We could distinguish the two parental alleles in each patient sample using informative SNPs (rs10732516 and rs2071094). The maternal allele, which is normally unmethylated, was completely methylated in the cord blood, peripheral blood, and skin from Patient 1. However, in placental samples from Patient 1, the maternal allele was only partially methylated: 36% of all CpGs analyzed were methylated. Similar results were observed in Patient 2: the maternal allele in the cord blood was 68% methylated; however, the maternal allele was only 31% and 55% methylated in the placenta and chorangioma samples, respectively. The paternal alleles, which are normally fully methylated, were fully methylated in all samples. These findings supported the results of the Southern blots. Furthermore, we could not find any microdeletions or mutations in or around H19-DMR,

including seven CTCF-binding sites, three OCT4 sites, and one SOX2 site, indicating that there was no genetic cause of the hypermethylation (Fig. 2A and data not shown).

Next, we analyzed polymorphic markers at 11p15.4–p15.5 to determine whether copy number abnormalities or paternal UPD might be involved in these BWS patients. Although smaller PCR products were more easily amplified, paternal–maternal allele ratios in blood samples were between 0.92 and 1.33, indicating that both parental alleles were equally represented in both patients (Fig. 2B). Therefore, we could rule out copy number abnormality and paternal UPD within the patients' blood. We also investigated maternal contamination in the placenta. *D11S1997* and *HUMTH01* for Patient 1 and the *RsaI* polymorphism in *H19* (rs2839703) for Patient 2 were used for this investigation because the mothers were expected to be homozygous for such polymorphisms. Thus, we investigated contamination of our samples by assessing the homozygosity of the polymorphisms in the mothers. The paternal–maternal ratios in Patient 1 were 0.94 and 1.03, indicating an equal contribution of both parental alleles and suggesting no contamination (Fig. 2B). In Patient 2, the ratios were 0.77 and 0.78 in the placenta and chorangioma, respectively, suggesting a small amount of contamination (Fig. 2C). However, such contamination was too

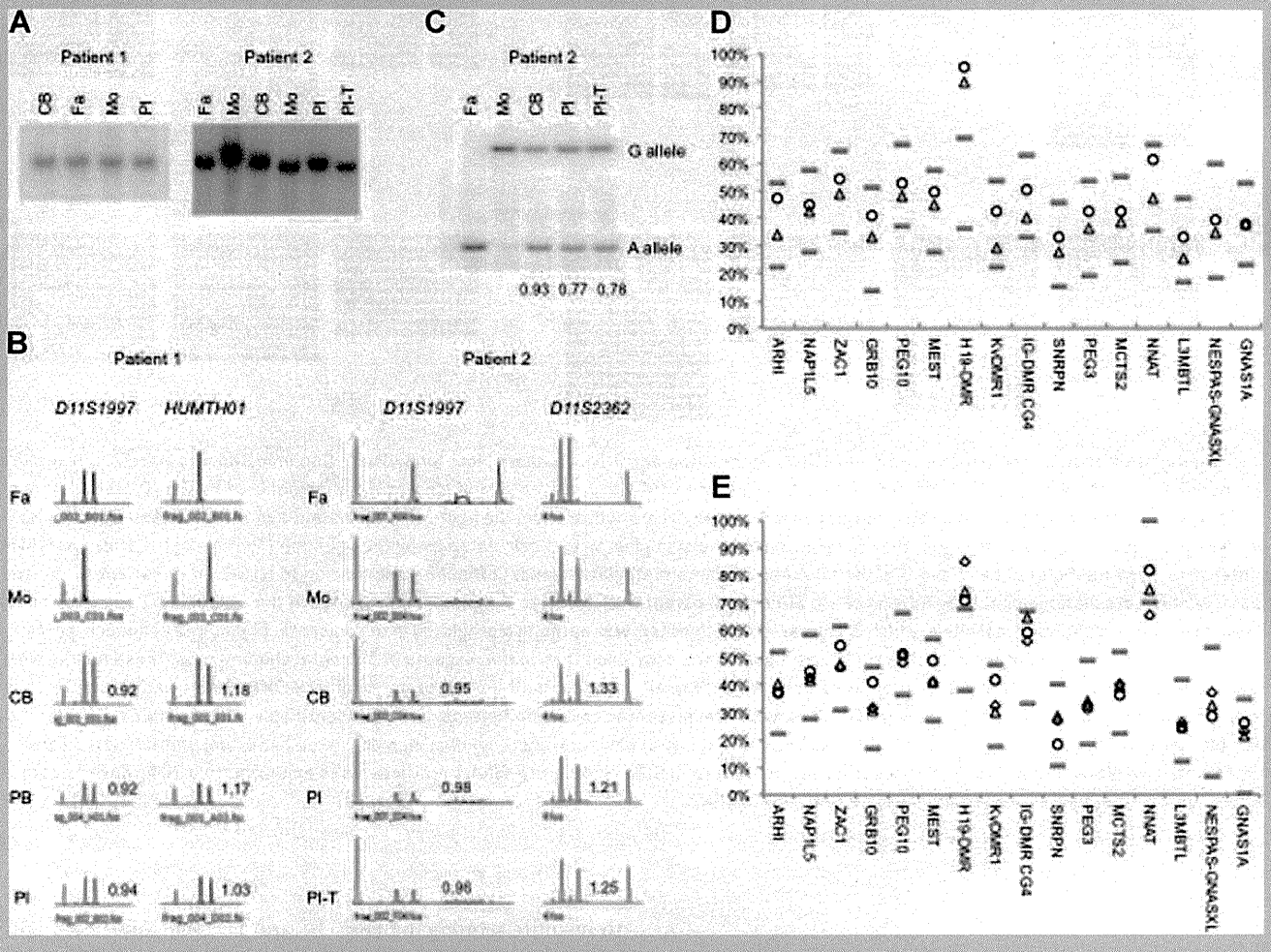

FIG. 2. Microdeletion analysis of H19-DMR, polymorphism analyses, and COBRA of primary imprinted DMRs in embryo-derived and placental samples. A: Southern blots identifying a microdeletion of H19-DMR. A genomic fragment (7.7 kb) generated by *ApaI* digestion, which included the entire H19-DMR, was evident in all samples, indicating that there was no microdeletion in this DMR. B: Microsatellite markers at 11p15.4–p15.5. The peak heights associated with each parental allele in all samples were quantitatively analyzed. The results indicated that both parental alleles were present and equally represented. C: Hot-stop PCR of an *RsaI* polymorphic site in Patient 2. The ratios of paternal allele to maternal allele are shown under the figure. Although the ratios in the placenta and placental chorangioma are lower than in the cord blood, suggesting a small amount of maternal contamination, this was not enough to affect the results of the methylation analyses. COBRA of cord blood (D) and placentas (E), demonstrating that H19-DMR was hypermethylated. CTS6 is contained within H19-DMR. Methylation at other DMRs was normal in all samples, except for methylation at NNAT, which was aberrant in the placental chorangioma. Cord blood and placentas from 24 normal individuals were used as controls. The upper limit of normal methylation was defined as the higher of these two values: (1) the average of controls + 3 SD, or (2) the average + 15%. Similarly, the lower limit of normal methylation was definite as the lower of these two values: (1) the average of controls − 3 SD, or (2) the average − 15%. The upper and lower limits are indicated by gray bars. ○: Patient 1; : Patient 2; ◇: placental chorangioma of Patient 2.

small to affect the results of the methylation analyses. In addition, sequence analysis did not show any mutations in *CDKN1C* (data not shown). These findings indicated that H19-DMR was aberrantly hypermethylated in both BWS patients and their associated placentas, but the aberrant methylation was consistently lower in the placenta, and that the H19-DMR GOM was strictly an isolated epimutation.

Finally, we analyzed the methylation status of 16 primary imprinted DMRs scattered throughout the genome-using COBRA (Fig. 2D and E). Only H19-DMR showed aberrant methylation among all primary DMRs in all samples, except for NNAT DMR, which was abnormal only in the placental chorangioma, indicating that the *IGF2/H19* imprinted domain was targeted for aberrant methylation in both somatic tissues and the placenta.

DISCUSSION

Methylation associated with parental imprints are erased in PGC and reestablished during gametogenesis in a sex-specific manner. The paternal pronucleus in the zygote undergoes active demethylation; extensive passive demethylation then ensues on maternal and paternal chromosomes during the pre-implantation period. After implantation, de novo methylation results in a rapid increase in DNA methylation in the inner cell mass (ICM), which gives rise to the entire embryo; in contrast, de novo methylation is either inhibited or not maintained in the trophoblast, which gives rise to the placenta [Li, 2002; Sasaki and Matsui, 2008]. The imprinted DMRs, however, escape these demethylation and de novo methylation events that occur in early embryogenesis. H19-DMR GOM in BWS patients is considered an error in imprint erasure in female PGCs [Horsthemke, 2010]. However, H19-DMR GOM, whether with or without microdeletions within H19-DMR, was partial, indicating a mosaic of normal cells and aberrantly methylated cells [Sparago et al., 2007; Cerrato et al., 2008]. These findings demonstrated that aberrant hypermethylation at H19-DMR was acquired after fertilization, although the precise timing was unknown.

Both participants in this study had isolated GOM at H19-DMR. The partial and variable hypermethylation among samples suggested epigenetic mosaicism. Furthermore, methylation levels in the placentas were lower than those in the blood and skin, suggesting that the aberrant methylation was acquired after implantation—when genome-wide de novo methylation normally occurs. Aberrant de novo methylation at H19-DMR is expected to be more widespread in the embryo than in the placenta, as this is normally the case for de novo methylation [Li, 2002; Sasaki and Matsui, 2008]; this disparity in efficiency could lead to the discordance between hypermethylation in trophoblast-derived placenta and that in embryo-derived blood and skin. This hypothesis is supported by a mouse experiment in which a mutant maternal allele harboring a deletion of four CTCF binding sites was hypomethylated in oocytes and blastocysts, yet was highly methylated after implantation [Engel et al., 2006]. To our knowledge, this is the first evidence demonstrating that aberrant hypermethylation of maternal H19-DMR is acquired after implantation in humans.

We found that of 16 primary imprinted DMRs analyzed, only H19-DMR showed aberrant methylation; even methylation at IG-DMR CG4, another paternally methylated, primary imprinted DMR, was normal in our patients. Although we only studied two patients, this finding indicated that the *IGF2/H19* imprinted domain in both the embryo and placenta was more susceptible than other imprinted domains to aberrant methylation acquired after implantation.

In conclusion, we found that methylation of H19-DMR was discordant in embryo-derived somatic tissue and placenta, strongly suggesting that the aberrant de novo methylation occurred after implantation. However, the precise mechanism of isolated H19-DMR GOM is still unknown. Since no mutations in *CTCF*, an important trans-acting imprinting factor, were found in these patients with isolated GOM at H19-DMR, the potential for mutations in the OCT and SOX transcription factors should be investigated because mutations of OCT-binding sites have previously been found in a few patients with H19-DMR GOM [Cerrato et al., 2008; Demars et al., 2010].

ACKNOWLEDGMENTS

This study was supported, in part, by a Grant-in-Aid for Scientific Research (C) (No. 20590330) from the Japan Society for the Promotion of Science, a Grant for Research on Intractable Diseases from the Ministry of Health, Labor, and Welfare, and a Grant for Child Health and Development from the National Center for Child Health and Development.

REFERENCES

Aoki A, Shiozaki A, Sameshima A, Higashimoto K, Soejima H, Saito S. 2011. Beckwith–Wiedemann syndrome with placental chorangioma due to H19-differentially methylated region hypermethylation: A case report. J Obstet Gynaecol Res 37:1872–1876.

Bell AC, Felsenfeld G. 2000. Methylation of a CTCF-dependent boundary controls imprinted expression of the Igf2 gene. Nature 405:482–485.

Cerrato F, Sparago A, Verde G, De Crescenzo A, Citro V, Cubellis MV, Rinaldi MM, Boccuto L, Neri G, Magnani C, D'Angelo P, Collini P, Perotti D, Sebastio G, Maher ER, Riccio A. 2008. Different mechanisms cause imprinting defects at the IGF2/H19 locus in Beckwith–Wiedemann syndrome and Wilms' tumour. Hum Mol Genet 17:1427–1435.

Demars J, Shmela ME, Rossignol S, Okabe J, Netchine I, Azzi S, Cabrol S, Le Caignec C, David A, Le Bouc Y, El-Osta A, Gicquel C. 2010. Analysis of the IGF2/H19 imprinting control region uncovers new genetic defects, including mutations of OCT-binding sequences, in patients with 11p15 fetal growth disorders. Hum Mol Genet 19:803–814.

Elliott M, Bayly R, Cole T, Temple IK, Maher ER. 1994. Clinical features and natural history of Beckwith–Wiedemann syndrome: Presentation of 74 new cases. Clin Genet 46:168–174.

Engel N, Thorvaldsen JL, Bartolomei MS. 2006. CTCF binding sites promote transcription initiation and prevent DNA methylation on the maternal allele at the imprinted H19/Igf2 locus. Hum Mol Genet 15:2945–2954.

Hark AT, Schoenherr CJ, Katz DJ, Ingram RS, Levorse JM, Tilghman SM. 2000. CTCF mediates methylation-sensitive enhancer-blocking activity at the H19/Igf2 locus. Nature 405:486–489.

Horsthemke B. 2010. Mechanisms of imprint dysregulation. Am J Med Genet C Semin Med Genet 154C:321–328.

Li E. 2002. Chromatin modification and epigenetic reprogramming in mammalian development. Nat Rev Genet 3:662–673.

Sasaki H, Matsui Y. 2008. Epigenetic events in mammalian germ-cell development: Reprogramming and beyond. Nat Rev Genet 9:129–140.

Sasaki K, Soejima H, Higashimoto K, Yatsuki H, Ohashi H, Yakabe S, Joh K, Niikawa N, Mukai T. 2007. Japanese and North American/European patients with Beckwith–Wiedemann syndrome have different frequencies of some epigenetic and genetic alterations. Eur J Hum Genet 15: 1205–1210.

Soejima H, Nakagawachi T, Zhao W, Higashimoto K, Urano T, Matsukura S, Kitajima Y, Takeuchi M, Nakayama M, Oshimura M, Miyazaki K, Joh K, Mukai T. 2004. Silencing of imprinted CDKN1C gene expression is associated with loss of CpG and histone H3 lysine 9 methylation at DMR-LIT1 in esophageal cancer. Oncogene 23:4380–4388.

Sparago A, Cerrato F, Vernucci M, Ferrero GB, Silengo MC, Riccio A. 2004. Microdeletions in the human H19 DMR result in loss of IGF2 imprinting and Beckwith–Wiedemann syndrome. Nat Genet 36:958–960.

Sparago A, Russo S, Cerrato F, Ferraiuolo S, Castorina P, Selicorni A, Schwienbacher C, Negrini M, Ferrero GB, Silengo MC, Anichini C, Larizza L, Riccio A. 2007. Mechanisms causing imprinting defects in familial Beckwith–Wiedemann syndrome with Wilms' tumour. Hum Mol Genet 16:254–264.

Uejima H, Lee MP, Cui H, Feinberg AP. 2000. Hot-stop PCR: A simple and general assay for linear quantitation of allele ratios. Nat Genet 25: 375–376.

Weksberg R, Nishikawa J, Caluseriu O, Fei YL, Shuman C, Wei C, Steele L, Cameron J, Smith A, Ambus I, Li M, Ray PN, Sadowski P, Squire J. 2001. Tumor development in the Beckwith–Wiedemann syndrome is associated with a variety of constitutional molecular 11p15 alterations including imprinting defects of KCNQ1OT1. Hum Mol Genet 10:2989–3000.

Weksberg R, Shuman C, Beckwith JB. 2010. Beckwith–Wiedemann syndrome. Eur J Hum Genet 18:8–14.

THE JOURNAL OF
Obstetrics and Gynaecology Research

doi:10.1111/j.1447-0756.2011.01654.x J. Obstet. Gynaecol. Res. Vol. 37, No. 12: 1872–1876, December 2011

Beckwith–Wiedemann syndrome with placental chorangioma due to H19-differentially methylated region hypermethylation: A case report

Aiko Aoki[1], Arihiro Shiozaki[1], Azusa Sameshima[1], Ken Higashimoto[2], Hidenobu Soejima[2] and Shigeru Saito[1]

[1]*Department of Obstetrics and Gynecology, University of Toyama, Toyama, and* [2]*Division of Molecular Genetics and Epigenetics, Department of Biomolecular Sciences, Faculty of Medicine, Saga University, Saga, Japan*

Abstract

Beckwith–Wiedemann syndrome (BWS) is a common overgrowth syndrome that involves abdominal wall defects, macroglossia, and gigantism. It is sometimes complicated by placental tumor and polyhydramnios. We report a case of BWS, prenatally diagnosed with ultrasonography. A large and well-circumscribed tumor also existed on the fetal surface of the placenta, which was histologically diagnosed as chorangioma after delivery. Polyhydramnios was obvious and the fetal heart enlarged progressively during pregnancy. Because the biophysical profiling score dropped to 4 points at 33 weeks of gestation, we carried out cesarean section. By epigenetic analysis, H19-differentially methylated region hypermethylation was observed in the placental tumor, normal placental tissue, and cord blood mononuclear cells. This is the first report of BWS with placental tumor due to H19-differentially methylated region hypermethylation.

Key words: Beckwith–Wiedemann syndrome, epigenetic abnormality, H19-differentially methylated region, hypermethylation, placental chorangioma, prenatal diagnosis.

Introduction

The incidence of Beckwith–Wiedemann syndrome (BWS) is estimated to be 1 in 13 700 deliveries.[1] BWS presents characteristic findings, genetic abnormalities, and a higher risk of malignancies. To our knowledge, there are only four reports of BWS with placental chorangioma, but no report was supported by epigenetic analysis. This is the first report of BWS with placental chorangioma, biallelic expression of *IGF2*, and reduced *H19* expression.

Case Report

A 27-year-old woman had an uneventful pregnancy (gravida 0, para 0) until 29 weeks of gestation. Assisted reproductive technology had not been performed. She complained of increased abdominal circumference and a sense of oppression at 29 weeks and 3 days into her pregnancy. Transabdominal sonography showed that the fetus was large for the gestational age. Additionally, a large and well-circumscribed placental tumor measuring about 12 cm in diameter and polyhydramnios were observed. She was diagnosed with preterm labor and was transferred to our hospital. Ultrasonography showed fetal macroglossia (Fig. 1a), enlargement of the liver (Fig. 1b) and the kidneys (Fig. 1c,d), and a large and well-circumscribed placental tumor (Fig. 1e). These clinical physical features suggested a prenatal diagnosis of BWS. Mild mitral and tricuspid regurgitation appeared in the fetal heart at 32 weeks of gestation, and became worse at 33 weeks of gestation. At 33 weeks and 5 days of gestation, biophysical profiling score was dropped to 4 points, and therefore a cesarean section

Received: February 3 2011.
Accepted: March 18 2011.
Reprint request to: Professor Shigeru Saito, Department of Obstetrics and Gynecology, University of Toyama, 2630 Sugitani, Toyama 930-0194, Japan. Email: s30saito@med.u-toyama.ac.jp

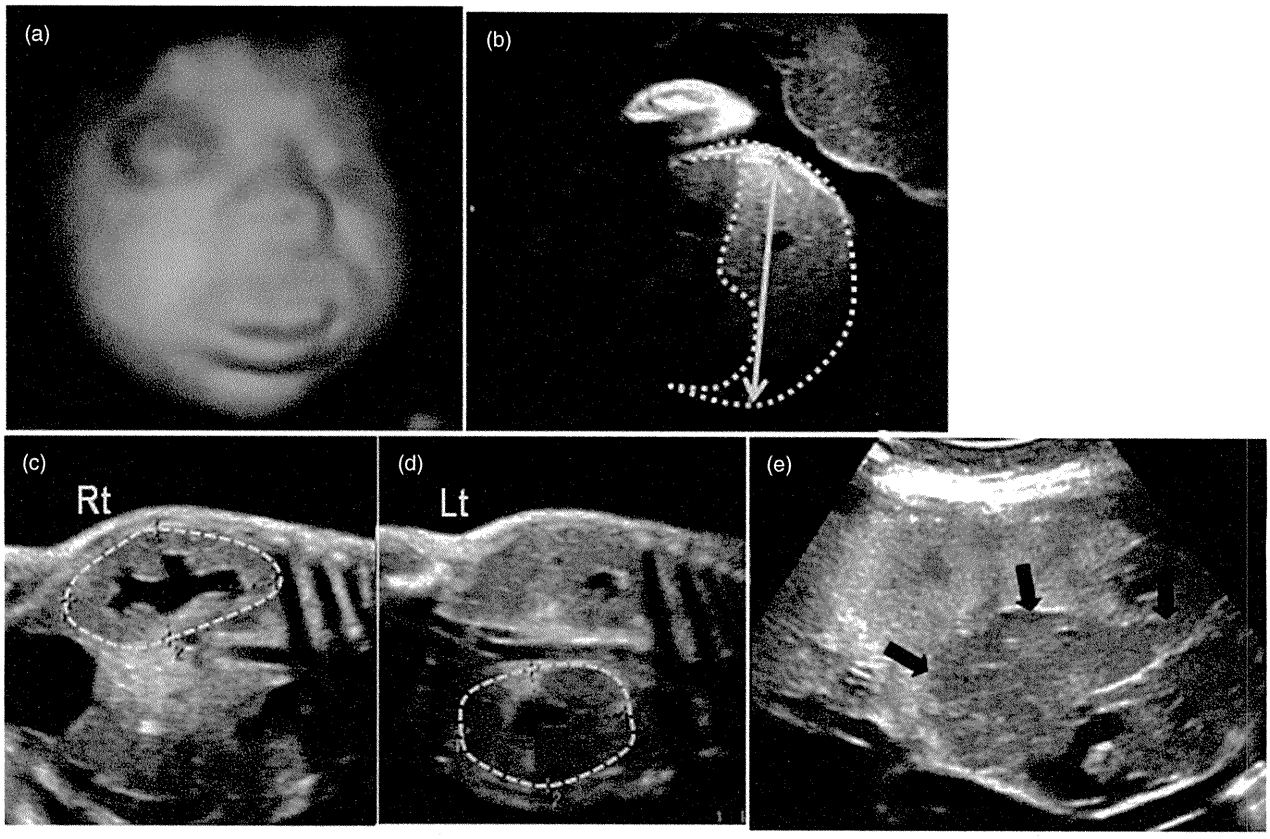

Figure 1 (a–e) Fetal and placental findings. Characteristic findings were seen using ultrasonography. (a) Macroglossia. (b) Hepatomegaly, measuring 87 mm (normal range at 29 weeks: 39 mm). (c,d) Enlarged kidneys, measuring 60 × 32 mm in right side, and 50 × 37 mm in the left side (normal range at 29 weeks: 28 × 15 mm). (e) A large, well-circumscribed tumor (12 cm in diameter) was found on fetal side of the placenta (arrows).

was performed for non-reassuring fetal status. The female baby weighed 2540 g and umbilical arterial blood pH was 7.127. Apgar scores were 3 and 7 points at 1 and 5 min, respectively. The baby had solitary, purple-red focuses on the body, macroglossia, and distended abdomen. Blood test showed hyperleukocytosis (32 520/mm^3), anemia (9.0 g/dL), thrombocytopenia (5.8×10^4/mm^3), and coagulopathy (Table 1). Blood transfusion was done for continuous anemia and low platelet count. For persistent neonatal hypoglycemia (around 20 mg/dL), steroid and glucose were used to keep the blood sugar level normal. Although mitral and tricuspid valve regurgitations existed, the cardiac function was stable. The fetal heart became progressively enlarged on the 8th postnatal day, and the baby suddenly died of cardiogenic shock on the 64th postnatal day (Fig. 2).

The weight of the placenta was 1620 g with a well-capsulated placental tumor measuring 12 cm on the fetal side of the placenta (Fig. 3a). Histological examination showed enlarged villi with an increased number of small blood vessels and the tumor was diagnosed with cellular placental chorangioma (Fig. 3b,c).

Table 1 Coagulopathy in the neonatal blood test

Prothrombin time	45.4 s
Prothrombin time %	<20
International normalized ratio	4.52
Activated partial thromboplastin time	>100 s
Fibrinogen	<50 mg/dL
Fibrin degenerative product	109.9 μg/mL
D-Dimer	35.0 μg/mL

The epigenetic analysis after delivery of the cord blood, placenta, and a part of the placental tumor showed H19-differentially methylated region (DMR)

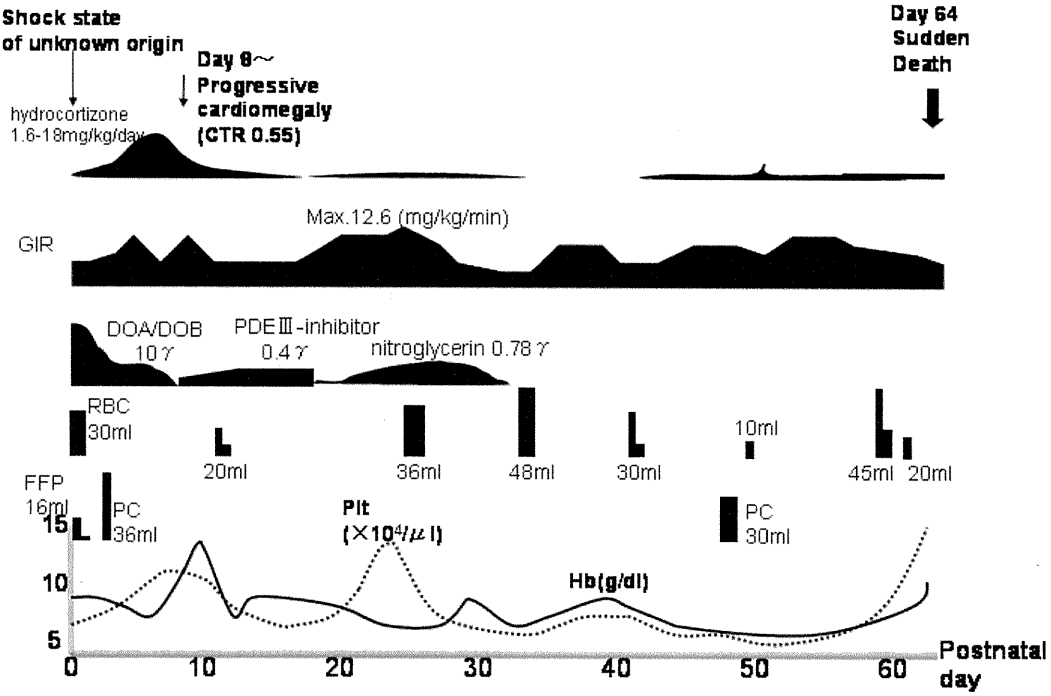

Figure 2 Neonatal clinical course. The baby went into a shock state 2 h after delivery, and was resuscitated with heart massage, cardiotonics and infusion of normal saline and sodium hydrogen carbonate. We performed a blood transfusion for continuous anemia and low platelet count. Because the glucose supply was not enough for persistent hypoglycemia, we administered steroids to keep the blood sugar level normal. The fetal heart was progressively enlarged on the 8th postnatal day, and the baby suddenly died of cardiogenic shock on the 64th postnatal day. CTR, cardiothoracic rate; DOA/DOB: dopamine/dobutamine; FFP, fresh frozen plasma; GIR, glucose infusion rate; Hb, hemoglobin; PC, platelet concentrates; PDE III-inhibitor, phosphodiesterase III inhibitor; Plt, platelet; RBC, red blood cell.

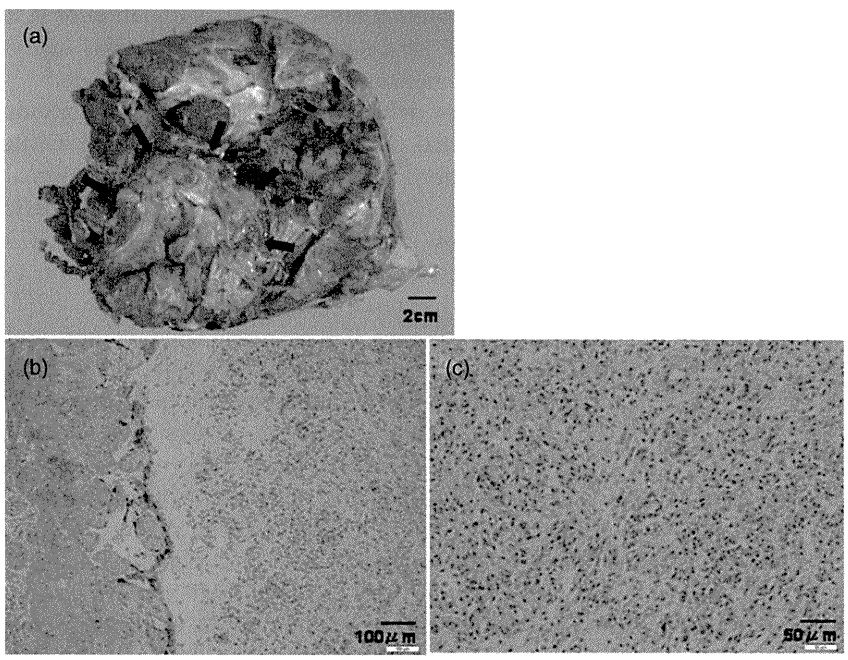

Figures 3 (a–c) Macroscopic and histological appearance of the placental tumor. (a) A well-circumscribed tumor (12.5 × 11.5 cm) was found on the fetal surface of the placenta (arrow). (b) Villi are enlarged and edematous (in the middle). (c) There is diffuse vascular proliferation in the enlarged villi, compatible with chorangioma.

hypermethylation. The parental blood tests showed no epigenetic abnormalities (Fig. 4). Another candidate methylation alteration site in BWS, KvDMR1, was normally methylated (data not shown). Genetic analyses ruled out paternal uniparental disomy of 11p15.5 and mutation of *CDKN1C* (data not shown).

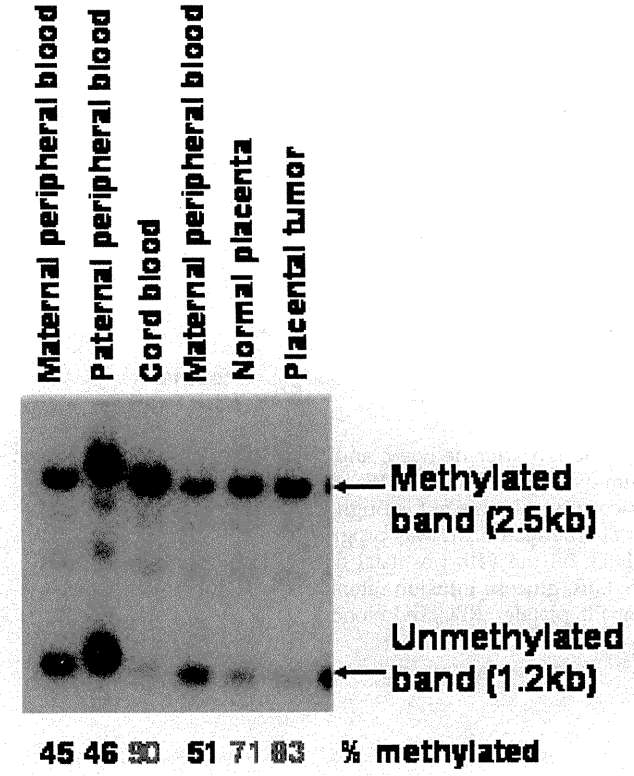

Figure 4 Epigenetic analysis. Quantity of H19-differentially methylated region (DMR) methylation status was determined by Southern blotting. Three micrograms of genomic DNA was digested with *Pst*I and methylation-sensitive *Mlu*I. The blot was probed by the PCR product, which was generated with a primer pair: 5′-CTCCGACTCCGTCTAAGGACA-3′ and 5′-GAGTGGAGACTGGCGAGTTTC-3′. KvDMR1 methylation status was also analyzed by Southern blotting with *Bam*HI and methylation-sensitive *Not*I. The blot was probed as previously described.[2] Band intensity obtained from Southern blotting was measured with a FLA-7000. The methylation index was calculated by (intensity of methylated band/[intensity of methylated band + intensity of unmethylated band]). H19-DMR hypermethylations are seen in the cord blood, normal placenta, and a part of the placental tumor (90%, 71%, 83%, respectively). Biallelic expression of *Igf2* and suppression of *H19* caused placentomegaly, macroglossia, visceromegaly and increased size for gestational age.

Discussion

Four BWS cases complicated with placental chorangioma have been reported,[3–6] but none was supported by epigenetic analysis. This is, to our knowledge, the first report proven to have epigenetic abnormality in BWS with placental chorangioma.

Chorangioma is asymptomatic when the size is smaller than 5 cm in diameter, but chorangiomas larger than 5 cm can cause some clinical problems, such as polyhydramnios, intrauterine fetal distress or death, fetal cardiac failure, neonatal anemia and thrombocytopenia, and disseminated intravascular coagulation, triggered by thromboplastic substances released from the small blood vessels in the chorangioma.[7] In our case, the tumor size was 12 cm and the features described above were observed.

Genomic imprinting is an epigenetic modification that inactivates one allele of a gene in a parent-of-origin-dependent manner.[8] Insulin-like growth factor 2 (*IGF2*)-*H19* imprinting control region (ICR), consisting of a methylation-sensitive chromatin insulator on chromosome 11p15.5, is responsible for epigenetic malformations in BWS.[9] In the *Igf2-H19* domain, especially in the placenta and tissues of endodermal origin, such as the liver, allele-specific gene expressions of parental origin are regulated by ICR located 2–4 kb upstream of the *H19* promoters. This region functions as a methylation-sensitive insulator that binds to CCCTC-binding factor (CTCF) on the unmethylated maternal allele. Alternatively, on the paternal allele, DNA methylation of ICR prevents CTCF binding, which permits access of the downstream enhancers to paternal *Igf2* promoters.[8]

In BWS cases, which have H19-DMR methylations in both paternal and maternal alleles (H19-DMR hypermethylation), the enhancers on the maternal allele activates *IGF2* promoters, leading to biallelic *IGF2* expression and the maternal copy of the *H19* gene is silenced because of expanded methylation to its promoter. Expression of imprinting gene, *IGF2*, depends on whether ICR is methylated or not, and loss of imprinting (LOI) of *IGF2* is associated with downregulation of *H19* expression, as previously reported.[10–12] Using epigenetic analysis, we could prove the existence of H19-DMR hypermethylation in the cord blood, placenta, and the placental tumor. Although we could not show biallelic *IGF2* expression because of homozygosity for *IGF2* polymorphism in the case (data not shown), H19-DMR hypermethylation would result in biallelic *IGF2* expression and associated reduced expression of *H19* due to the

reason mentioned above. In view of the potential function of *IGF2-H19*, these conditions led to cell proliferation and caused clinical appearances, such as macroglossia, visceromegaly (increased abdominal circumference), and the placental tumor. We explained to the mother that an occasional epigenetic abnormality (H19-DMR hypermethylation) caused BWS in the baby and that it would be extremely rare to recur in the next pregnancy.

References

1. Thorburn MJ, Wright ES, Miller CG, Smith-Read EH. Exomphalos-macroglossia-gigantism syndrome in Jamaican infants. *Am J Dis Child* 1970; **119**: 316–321.
2. Mitsuya K, Meguro M, Lee MP *et al. LIT1*, an imprinted antisense RNA in the human *KvLQT1* locus identified by screening for differentially expressed transcripts using monochromosomal hybrids. *Hum Mol Genet* 1999; **8**: 1209–1217.
3. Lage JM. Placentomegaly with massive hydrops of placental stem villi, diploid DNA content, and fetal omphaloceles: possible association with Beckwith–Wiedemann syndrome. *Hum Pathol* 1991; **22**: 591–597.
4. Drut RM, Drut R. Nonimmune fetal hydrops and placentomegaly: diagnosis of familial Wiedemann-Beckwith syndrome with trisomy 11p15 using FISH. *Am J Med Genet* 1996; **62**: 145–149.
5. Takayama M, Soma H, Yaguchi S *et al.* Abnormally large placenta associated with Beckwith–Wiedemann syndrome. *Gynecol Obstet Invest* 1986; **22**: 165–168.
6. Drut R, Drut RM, Toulouse JC. Hepatic hemangioendotheliomas, placental chorioangiomas, and dysmorphic kidneys in Beckwith–Wiedemann syndrome. *Pediatr Pathol* 1992; **12**: 197–203.
7. Fox H. Non-trophoblastic tumors of the placenta. In: Fox H (ed.). *Obstetrical and Gynecological Pathology*, 3rd edn. Philadelphia: Churchill Livingstone, 1987; 1030–1044.
8. Fowden AL, Sibley C, Reik W, Constancia M. Imprinted genes, placental development and fetal growth. *Horm Res* 2006; **65** (Suppl 3): 50–58.
9. Choufani S, Shuman C, Weksberg R. Beckwith–Wiedemann syndrome. *Am J Med Genet C Semin Med Genet* 2010 **154C**: 343–354.
10. Steenman MJ, Rainier S, Dobry CJ, Grundy P, Horon IL, Feinberg AP. Loss of imprinting of *IGF2* is linked to reduced expression and abnormal methylation of *H19* in Wilms' tumour. *Nat Genet* 1994; **7**: 433–439.
11. Bell AC, Felsenfeld G. Methylation of a CTCF-dependent boundary controls imprinted expression of the *Igf2* gene. *Nature* 2000; **405**: 482–485.
12. Hark AT, Schoenherr CJ, Katz DJ, Ingram RS, Levorse JM, Tilghman SM. CTCF mediates methylation-sensitive enhancer-blocking activity at the *H19/Igf2* locus. *Nature* 2000; **405**: 486–489.

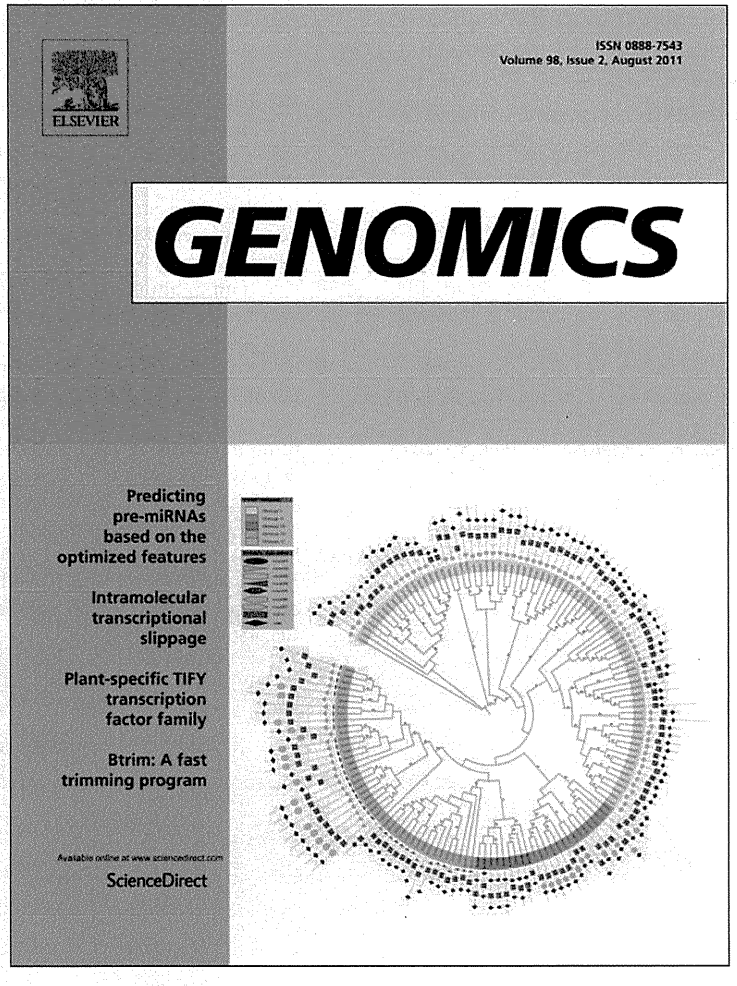

Genomics 98 (2011) 120–127

Contents lists available at ScienceDirect

Genomics

journal homepage: www.elsevier.com/locate/ygeno

Methylation dynamics of IG-DMR and *Gtl2*-DMR during murine embryonic and placental development

Shun Sato [a], Wataru Yoshida [a], Hidenobu Soejima [b], Kazuhiko Nakabayashi [a,*], Kenichiro Hata [a]

[a] *Department of Maternal-Fetal Biology, National Research Institute for Child Health and Development, Tokyo 157-8535, Japan*
[b] *Division of Molecular Genetics and Epigenetics, Department of Biomolecular Sciences, Faculty of Medicine, Saga University, Saga 849-8501, Japan*

ARTICLE INFO

Article history:
Received 5 December 2010
Accepted 12 May 2011
Available online 18 May 2011

Keywords:
Genomic imprinting
DNA methylation
IG-DMR
Gtl2-DMR

ABSTRACT

The *Dlk1-Dio3* imprinted domain on mouse chromosome 12 contains IG-DMR and *Gtl2*-DMR, whose methylation patterns are established in the germline and after fertilization, respectively. In this study, we determine that acquisition of DNA methylation at the paternal allele of the *Gtl2*-DMR is initiated after the blastocyst stage and completed by embryonic day 6.5, and that *Gtl2* (approved symbol: Meg3) is monoallelically expressed from the maternal allele as early as the blastocyst. Therefore, DNA methylation at the *Gtl2*-DMR is not a prerequisite for the imprinted expression of *Gtl2*, which may be involved in the control of proliferation and differentiation of cells during early gestation. We also reveal that a subregion of the IG-DMR exhibits tissue-specific differences in allelic methylation patterns. These results add to the growing body of knowledge elucidating the mechanism whereby parent-of-origin-dependent DNA methylation at the IG-DMR leads to the imprinted expression of the *Dlk1-Dio3* cluster.

1. Introduction

Genomic imprinting is an epigenetic mechanism that regulates transcription, whereby the expression of a subset of genes is limited to or biased towards one parental allele. To date, over one hundred imprinted genes have been identified in the mouse (http://www.har.mrc.ac.uk/research/genomic_imprinting). Imprinted genes tend to be clustered on the genome. One of the common features among imprinted loci is that such genomic intervals include one or more differentially methylated regions (DMRs), which exhibit parent-of-origin dependent DNA methylation patterns [1]. DMRs have been classified into two types according to the time at which their DNA methylation patterns are established. Primary (germline) DMRs harbor allelic DNA methylation inherited from the male or the female gamete. Secondary (post-zygotic) DMRs acquire parent-of-origin dependent methylation patterns after fertilization. In mice, germline DMRs are shown to be established during the oocyte growth stage (postnatal days 5 to 20) [2,3] or the prospermatogonia stage (embryonic days 14.5 to newborn) [4–6] by a DNMT3L-dependent mechanism [7–12]. Several germline DMRs have been shown to govern the imprinted expression of genes as well as the methylation of post-zygotic DMRs within chromosomal regions. These germline DMRs, known as imprinting control regions (ICRs), regulate these regions by *cis*-acting mechanisms. [13–15]. On the other hand, little is known about the function of secondary DMRs in the regulation of imprinted gene expression, as well as *cis*-acting mechanisms and *trans*-acting factors that establish DNA methylation at secondary DMRs.

Studies focusing on the regulatory functions of ICRs have revealed a number of different molecular mechanisms that underlie the coordinated and long-range regulation of imprinted genes. In the *H19/Igf2* domain, long range chromatin interactions mediated by CTCF between the primary *H19*-DMR and the secondary *Igf2*-DMRs play an integral role in the regulation of imprinted gene expression at this locus [13,16]. Another mechanism involves non-coding (nc) RNAs such as *Airn* in the *Igf2r* locus and *Kcnq1ot1* in the *Kcnq1* imprinted gene cluster. These ncRNAs are transcribed from ICRs and are shown to be functionally linked to the silencing of genes in *cis* through gene- and lineage-specific repressive chromatin modifications [14,17,18]. These two mechanisms are likely to be involved in the regulation of many other imprinted loci as well. However, the sequence of events leading to the establishment and maintenance of imprinted expression for a cluster of genes remains largely elusive for many imprinted loci.

The *Dlk1-Dio3* imprinting cluster on mouse distal chromosome 12 contains the intergenic germline-derived DMR (IG-DMR) and the *Gtl2*-DMR, whose methylation patterns are established in the germline and after fertilization, respectively [19,20]. The cluster consists of at least three paternally expressed protein-coding genes (*Dlk1*, *Rtl1*, and *Dio3*), and four maternally expressed ncRNAs (*Gtl2*, *Anti-Rtl1*, *Rian* and *Mirg*). The IG-DMR is shown to function as the ICR of this imprinted gene cluster [15,21]. A targeted disruption study of the IG-

* Corresponding author at: Department of Maternal-Fetal Biology, National Research Institute for Child Health and Development, 2-10-1 Okura, Setagaya, Tokyo 157-8535, Japan. Fax: +81 3 3417 2864.
E-mail address: knakabayashi@nch.go.jp (K. Nakabayashi).

0888-7543/$ – see front matter © 2011 Elsevier Inc. All rights reserved.
doi:10.1016/j.ygeno.2011.05.003

DMR [15] has revealed that the maternally inherited IG-DMR, which is unmethylated, is essential in the embryo to maintain the unmethylated status of the *Gtl2*-DMR, the expression of the ncRNAs, and the repression of the protein-coding genes, on the maternal allele. However, the principal mechanism whereby the allele-specific methylation at the IG-DMR leads to the imprinted expression of the cluster of genes on chromosome 12 is unknown. It has been also demonstrated that, in the placenta, the absence of the maternally inherited IG-DMR results in the activation of protein-coding genes but only partial repression of the ncRNAs, and leads to no phenotypic consequence [21]. Therefore, mechanisms underlying the imprinted expression of the maternally-expressed ncRNAs are different between the embryonic and the extra-embryonic tissue lineages.

Among known secondary DMRs, the *Gtl2*-DMR is unique in that it has been demonstrated to possess an essential long-range imprinting regulatory function. A neonatal patient showing a paternal uniparental disomy 14-like phenotype in the body but not in the placenta was identified to have a maternally-inherited heterozygous microdeletion that encompasses the *MEG3*-DMR (the human orthologue of the mouse *Gtl2*-DMR) but not the IG-DMR. In this patient, the maternal allele of *DLK1* has been shown to be reactivated [22]. Recent studies have used knockout mouse models with targeted deletions of the *Gtl2* locus, spanning the *Gtl2*-DMR. These studies have also suggested that *Gtl2* and/or *Gtl2*-DMR could regulate the expression of maternally expressed genes, indicating that the methylation of the *Gtl2*-DMR is a critical element in the *Dlk1-Dio3* imprinted domain [23,24]. In light of the critical roles that *Gtl2* and *Gtl2*-DMR may play in the imprinted regulation of this region, understanding the epigenetic mechanisms that govern them during early development is expected to further elucidate the mechanisms regulating the *Dlk1-Dio3* imprinted domain.

Recently, Stadtfeld et al. [25] reported that mouse induced pluripotent stem cells (iPSC) with repressed expression of maternally expressed ncRNAs in the *Dlk1-Dio3* domain contributed poorly to chimeras and failed to generate all-iPSC mice. In contrast, iPSCs with normal ncRNA expression patterns contributed to high-grade chimeras and produced all-iPSC mice. Hypermethylation of both the IG-DMR and the *Gtl2*-DMR was found to be associated with the reduced expression of ncRNAs in the iPSCs exhibiting poor contribution to chimeras [25]. This epimutation is considered to be caused by the iPSC reprogramming, rather than existing aberrant methylation patterns in the DMRs of the somatic cell of origin [25]. Therefore, a better understanding of the epigenetic regulation of these DMRs may eventually lead to improved reprogramming strategies of iPSC.

In this study, we determined the allelic DNA methylation patterns at the IG-DMR and the *Gtl2*-DMR, as well as the allelic expression patterns of *Dlk1* and *Gtl2* at early developmental stages (embryonic days 3.5 to 7.5) in embryonic and extra-embryonic tissues.

2. Results

2.1. Developmental dynamics of allelic DNA methylation patterns at IG- and Gtl2-DMRs in sperm, blastocysts, and post-implantation embryos

We examined allelic DNA methylation patterns at the IG-DMR and the *Gtl2*-DMR in whole embryos at embryonic day 3.5 (E3.5) and E5.5 as well as their methylation status in sperm. We regarded the genomic intervals defined by Kobayashi et al. [26] and Takada et al. [20] as the IG-DMR and the *Gtl2*-DMR, respectively. Three regions within the IG-DMR and the two regions within the *Gtl2*-DMR were chosen as targets for bisulfite sequencing (Fig. 1A). All five regions contain at least one single nucleotide polymorphism (SNP) between C57BL/6 (B6) and JF1/Ms (JF1) strains that can distinguish parental alleles in F1 hybrid materials (see details in Section 4.2 in the Materials and methods).

The IG-DMR was heavily methylated in all three regions (methylation percentage 81.3–95.8%) in sperm (Fig. 1B) as shown previously [20]. In blastocysts (E3.5), all three regions within the IG-DMR were maternally unmethylated (0–1.8%), yet paternally methylated (43.1–71.8%) (Fig. 1B). The observed levels of paternal methylation at E3.5 were significantly lower than those observed in sperm, implying that the paternal IG-DMR partially loses methylation at CpG dinucleotides after fertilization. This loss of methylation may be caused by the active and the passive demethylation of the paternal genome in pronucleus and preimplantation embryos, respectively [27,28]. At E5.5, the maternal allele of IG-DMR was found to be hypomethylated (1.9–18.3%), and the paternal allele to be hypermethylated (80.2–91.4%; Fig. 1B). The methylation level of the paternal allele was consistently higher at E5.5 than at E3.5. Additionally, it was almost fully methylated at E5.5 in all three regions examined, suggesting that de novo methylation events occur on the paternal allele of the IG-DMR during the developmental period between E3.5 and E5.5. These are the first results to illustrate the developmental dynamics of paternal methylation levels at the IG-DMR around the implantation period.

The differential methylation of the *Gtl2*-DMR on the paternal allele has been shown to be established in E13.5 embryos [20]. However, the post-zygotic stages at which the region's paternal methylation is initiated and completed remain unknown. Additionally, the relationship between the imprinted expression of *Gtl2* and DNA methylation at the *Gtl2*-DMR has not been elucidated. We confirmed that the *Gtl2*-DMR was unmethylated in sperm, and found that it was unmethylated on both parental alleles in blastocysts (Fig. 1B). In E5.5 embryos, the maternal allele remained hypomethylated (6.0 and 11.7%), while the paternal allele became partially methylated (55.2% in R4 and 42.7% in R5 regions) (Fig. 1B). In E6.5 and E7.5 embryos, the paternal allele of the *Gtl2*-DMR was found to be heavily methylated (75.8% or higher) (Fig. 1C). These data demonstrate that paternal methylation of the *Gtl2*-DMR is initiated after the blastocyst stage and is completed by E6.5 stage in the embryonic lineage.

2.2. Allelic DNA methylation patterns at IG- and Gtl2-DMRs in early and late gestational stages

It has been reported that, in both human and mouse placenta, the IG-DMR maintains its allele-specific methylation patterns, whereas the *Gtl2*-DMR does not show differential methylation between parental alleles [21,29,30]. To determine the developmental stage at which the allelic methylation patterns at the *Gtl2*-DMR diverge between embryonic and extra-embryonic lineages, we examined the DNA methylation status of the *Gtl2*-DMR as well as the IG-DMR in E6.5 and E7.5 tissues. In extra-embryonic tissues at both E6.5 and E7.5 stages, the *Gtl2*-DMR was partially methylated on both parental alleles, whereas its differential methylation was well maintained in embryonic tissues (Fig. 1C). The *Gtl2*-DMR was previously shown to be partially methylated on both parental alleles in late gestation (E16.5) placentas [21,29]. Our results demonstrate that the allelic methylation pattern observed in E16.5 placenta is already present in the extra-embryonic lineage at E6.5 stage.

Unexpectedly, we observed loss of differential methylation at the R2 and R3 regions within the IG-DMR in extra-embryonic tissues, although the R1 region maintained its differential methylation. The loss of differential methylation was more evident in E7.5 stage than in E6.5 stage (Fig. 1C). To assess whether the loss of differential methylation at the R2/R3 regions as well as the R4/R5 regions was specific to the extra-embryonic lineage, we examined the allelic methylation patterns of the R1–R5 regions in fetal tissues from late gestation time points. E16.5 skeletal muscle, E15.5 brain, and E16.5 liver were analyzed since they represent tissues derived from the

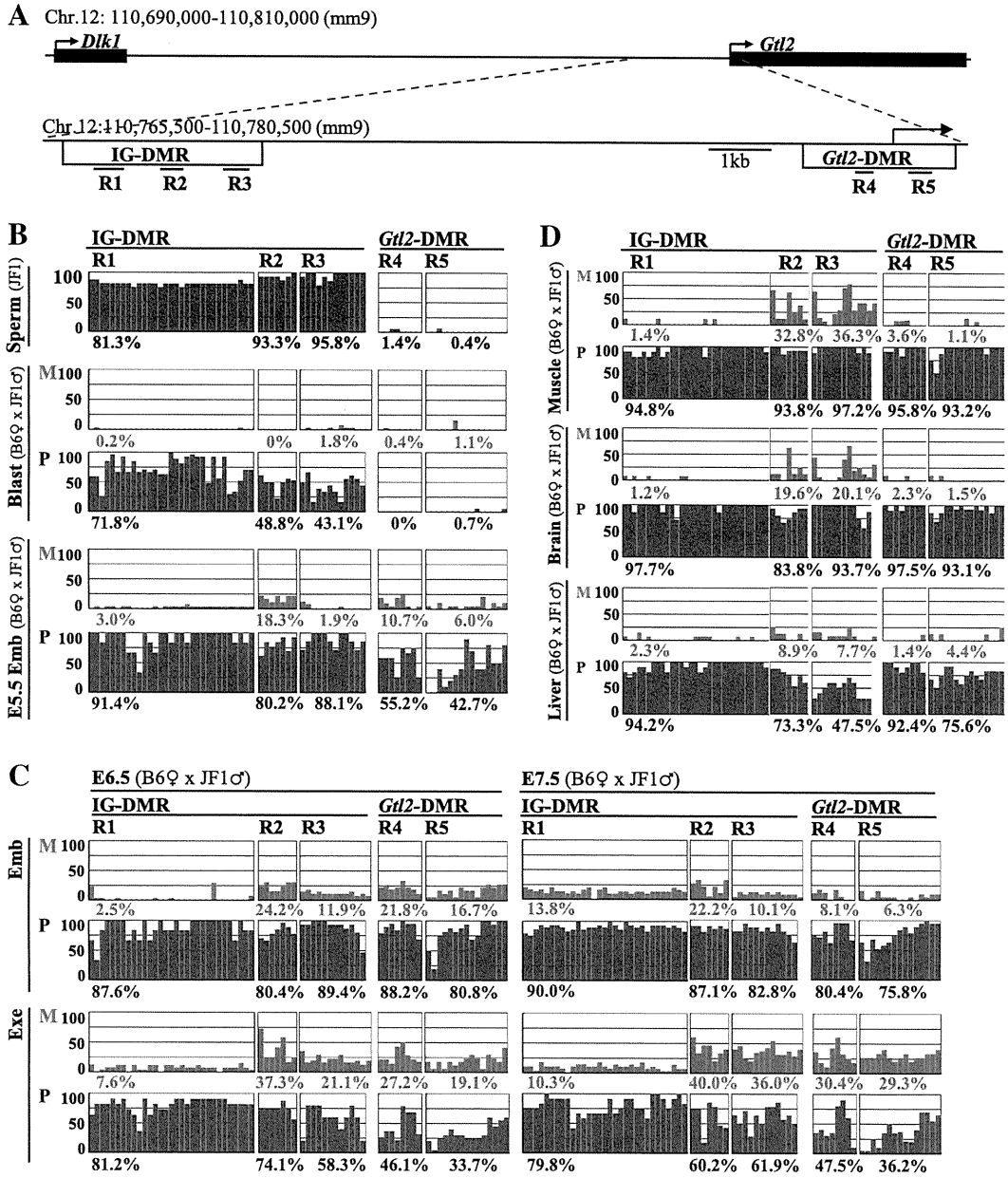

Fig. 1. Allelic DNA methylation patterns at the IG-DMR and the *Gtl2*-DMR during embryonic and extra-embryonic development. (A) A schematic diagram of the locus containing the IG-DMR and the *Gtl2*-DMR (shown as open boxes). The bars under the open boxes indicate the regions (R1–R5) analyzed by bisulfite sequencing. The arrow indicates the transcription start site of *Gtl2*. Scale bar = 1 kb. (B–D) Graphical representation of the methylation percentage at each CpG site in sperm, blastocysts at E3.5 (Blast), and embryos at E5.5 (E5.5_Emb) (B), in embryonic (Emb) and extra-embryonic (Exe) tissues at E6.5 and E7.5 (C), and in fetal tissues (E16.5 skeletal muscle, E15.5 brain, and E16.5 liver) (D). The vertical bars represent the percentage ratio of methylated cytosine at each CpG site, which were determined from the data of clone-based bisulfite sequencing (Supplementary Fig. 1). Overall methylation percentage for each region (the number of methylated CpGs per the number of total CpGs) is shown under each panel. As described in the Materials and Methods (Section 4.2), methylation percentage for each CpG site and each region was calculated using bisulfite sequencing data for a single sample (sperm and E15.5/16.5 fetal tissues) or two independent samples (E3.5 to E7.5 samples). M and P denote maternal and paternal alleles, respectively.

mesoderm, the ectoderm, and the endoderm, respectively. We found that differential methylation at the R1 region of the IG-DMR and the R4/R5 region of the *Gtl2*-DMR was strictly conserved. In contrast, differential methylation at the R2/R3 regions of the IG-DMR was partially lost to varying degrees in these tissues (Fig. 1D). Partial gain of methylation on the maternal allele (most notably observed in skeletal muscle) and partial loss of methylation on the paternal allele (most remarkably observed in the liver) were detected. Taken together, our data demonstrate that only a subregion of the IG-DMR containing the R1 region strongly maintains allele-specific differential methylation during embryonic development, whereas the rest of region containing the R2/R3 regions exhibits various tissue-specific allelic methylation patterns.

2.3. Allelic expression patterns of Dlk1 and Gtl2 during embryonic and extra-embryonic development

We subsequently assessed the expression levels and the allelic expression patterns of *Dlk1* and *Gtl2*. Although the expression of *Gtl2* is shown to be detectable as early as the pre-implantation stage [31], previous studies have not assessed the expression levels of these genes in a quantitative manner and have not determined their allelic expression patterns during early gestation (E3.5 to 7.5). Therefore, we performed both quantitative RT-PCR and pyrosequencing to quantify the allelic expression of these transcripts.

To determine the relative expression levels of *Gtl2* and *Dlk1*, quantitative RT-PCR was performed using E3.5 to E7.5 tissues and

E16.5 skeletal muscle tissues. The E16.5 skeletal muscle was chosen as a reference tissue for the relative expression levels of *Dlk1* and *Gtl2* because both transcripts have been shown to be highly expressed in E14.5 to E18.5 skeletal muscle [19,20,31]. We obtained the Ct (cycle threshold) values of *Gtl2* in E5.5–7.5 tissues (23.2 to 33.5) within the Ct value range of the standard curve for *Gtl2* (20.0 to 35.3), and determined the relative expression levels of *Gtl2* in these tissues, ranging from 0.0036 (E7.5Exe) to 0.31 (E6.5Exe) relative to the average level of E16.5 skeletal muscle samples (Fig. 2A). As demonstrated by Schuster-Gossler et al. [31], we were consistently able to detect the expression of *Gtl2* in blastocysts in our replicate samples, and determined its average relative expression level to be 0.011. However, this value should be considered with caution because the Ct values of the blastocyct samples (35.9, 36.4, and 36.5) were slightly out of range. Our results demonstrate that *Gtl2* is expressed at low levels at E3.5, up-regulated transiently at E5.5 and E6.5, and down-regulated at E7.5. Variation in the relative expression levels of *Gtl2* among three replicate samples was most remarkable in extra-embryonic tissues at E6.5. Because *Gtl2* expression seems to decrease rapidly between E6.5 and E7.5 in extra-embryonic tissues, subtle differences in the developmental stage among our E6.5 samples may account for the variation in *Gtl2* expression levels.

We obtained the Ct values of *Dlk1* in E5.5–7.5 tissues (26.5 to 35.4) within the Ct value range of the standard curve for *Dlk1* (21.6 to 36.8), and determined that the relative expression levels of *Dlk1* in these tissues ranged from 0.00021 (E7.5Exe) to 0.015 (E7.5Emb). The expression of *Dlk1* was undetectable in the blastocyst samples, and was consistently low in E5.5–7.5 tissues. In embryonic tissues, *Dlk1* expression levels tended to increase as embryonic development progressed (Fig. 2A). These results represent the first quantitative measurement of *Gtl2* and *Dlk1* expression levels during early gestational stages. The transient up-regulation of *Gtl2* around E5.5 and E6.5 stages suggest a possible role of this ncRNA in the control of growth and differentiation at these developmental stages.

To complete our analysis of the allelic expression patterns of *Glt2* and *Dlk1*, we quantitatively measured the allelic expression levels of these transcripts by pyrosequencing. *Gtl2* was consistently found to be

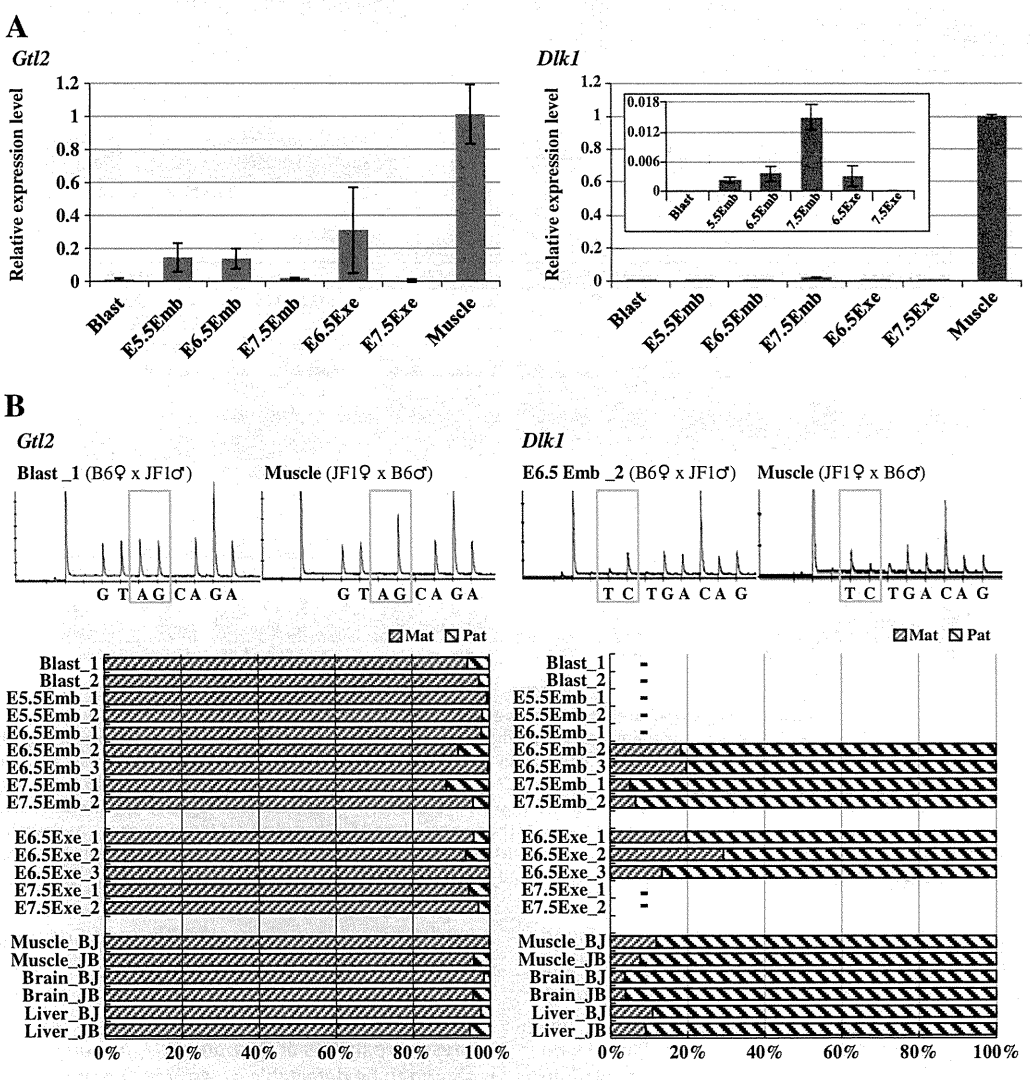

Fig. 2. Expression analysis of *Gtl2* and *Dlk1* during embryonic and extra-embryonic development. (A) Graphical representation of the relative expression levels of *Gtl2* and *Dlk1* in embryonic and extra-embryonic tissues at E3.5 to E7.5. The bars represent the mean expression levels of replicate samples relative to the mean expression level of E16.5 muscle samples (n = 4). Error bar = standard deviation (SD). The mean ± SD of each sample set for *Gtl2*: Blast, 0.011 ± 0.0094; E5.5Emb, 0.14 ± 0.088; E6.5Emb, 0.14 ± 0.061; E7.5Emb, 0.018 ± 0.0033; E6.5Exe, 0.31 ± 0.26; E7.5Exe, 0.0036 ± 0.0095. The mean ± SD for *Dlk1*: E5.5Emb, 0.0023 ± 0.00066; E6.5Emb, 0.0035 ± 0.0016; E7.5Emb, 0.015 ± 0.0025; E6.5Exe, 0.0030 ± 0.0021; E7.5Exe, 0.00021 ± 0.00015. (B) Quantitative allelic expression analysis of *Gtl2* and *Dlk1* by pyrosequencing. The top panels show examples of pyrograms. The yellow box in each pyrogram denotes the peaks at SNPs between the B6 and the JF1 strains. The alleles (B6/JF1) of SNPs are A/G for *Gtl2* and T/C for *Dlk1*. The bottom panels represent the allelic expression ratios of the paternal (Pat, blue stripe) and the maternal (Mat, red stripe) alleles. "–" in the panel for *Dlk1* indicates that the corresponding sample was not analyzed due to the absence or low expression of *Dlk1*.